

Check for updates



An integrated longitudinal and lateral control of vehicle platoons

Proc IMechE Part D:

J Automobile Engineering
1–17

Image: IMechE 2024
Image: I

Shuyou Yu^{1,2}, Yajing Zhang¹, Yunyong Li¹, Hong Chen^{1,3} and Baojun Lin⁴

Abstract

This paper proposes an integrated longitudinal and lateral control scheme for a vehicle platoon with the predecessor-leader communication topology. Both longitudinal and lateral dynamics are established, where the lateral dynamics considers the influence of variance of the longitudinal velocity. The decoupled longitudinal and lateral controllers are designed, respectively. The longitudinal controller adopts the distributed model predictive control algorithm, which regulates the following vehicles to track the longitudinal velocity of the leading vehicle and to keep the inter-vehicle desired spacing. Both the recursive feasibility of optimization problem and the asymptotic consensus of vehicle platoons are analyzed. Furthermore, the lateral controller adopts a feedforward and robust feedback control strategy to track the reference path without offset of the lateral position error. Simulation results in joint of MATLAB/Simulink and TruckSim verify the effectiveness of the proposed scheme.

Keywords

Platoon control, distributed control, model predictive control, robust control, time-varying systems

Date received: 16 January 2024; accepted: 3 September 2024

Introduction

Recently, platoon control of automated and connected vehicles has gained widespread attention because of its ability to increase road safety, improve traffic efficiency, and decrease fuel consumption.^{1,2} The control objective of a platoon is that each vehicle follows a reference path with a desired velocity according to a preset inter-vehicle spacing. Furthermore, the actual road is not always straight, that is, the vehicle platoons not only require longitudinal control but also lateral control. Therefore, the control objective can be divided into two tasks: the longitudinal control maintains the consensus of a platoon by adjusting the velocity of the following vehicles³; the lateral control minimizes the lateral error to achieve the vehicles traveling along the centerline of the designed lane.⁴

In previous work, many methods have been proposed to design longitudinal controllers of vehicle platoons, such as PID control, 5,6 H_{∞} control, 7 distributed sliding mode control, 8 distributed model predictive control (DMPC), 9 etc. DMPC scheme has been widely used because of its advantages of multi-objective optimization and explicit handling of constraints. 10,11 The DMPC strategy is proposed based on different performance requirements, including security, stability, and

feasibility analysis.^{12–15} A DMPC scheme is presented for a platoon consisting of vehicles with model uncertainty and disturbance.¹³ A DMPC scheme with input constraints is proposed for vehicle platoons to ensure smooth changes in control inputs for following the velocity of preceding vehicle.¹⁴ By virtue of the Lagrangian multiplier method and the dual decomposition technique, a DMPC method is proposed for vehicle platoons with coupled safety inter-vehicle distance constraints.¹⁵ Furthermore, the terminal equality constraint is used to guarantee consensus of platoon.^{3,16,17} A DMPC approach is proposed for heterogeneous

Corresponding author:

Shuyou Yu, Department of Control Science and Engineering, Jilin University, No.5988, Renmin Street, Changchun 130012, China. Email: shuyou@jlu.edu.cn

¹Department of Control Science and Engineering, Jilin University, Changchun, China

²The Key Laboratory of Industrial Internet of Things and Networked Control, Chongqing University of Posts and Telecommunications, Chongqing, China

³College of Electronics & Information Engineering, Tongji University, Shanghai, China

⁴Electrical and Electronic Teaching Center, Jilin University, Changchun, China

vehicle platoons, which imposes a terminal equality constraint such that the terminal state of each following vehicle is forced to be mean of the state of its communicating vehicle so as to ensure consensus of the platoon.¹⁶ A DMPC scheme for vehicle platoons is proposed, where a terminal equality constraint is imposed to ensure the asymptotic consensus of platoons.3 A DMPC strategy is developed for vehicle platoons under switching communication topologies, where the convergence of the platoon is proved based on a terminal equality constraint.¹⁷ In general, the terminal equality constraint is conservative. Therefore, the terminal inequality constraint is proposed to guarantee the recursive feasibility of the optimization problem and to achieve the asymptotic consensus of the platoons. 18-20 A dual-mode DMPC strategy is proposed for vehicle platoons to reduce the computation time and save communication resources. 19 A DMPC scheme with terminal inequality constraints is adopted for a platoon, where an improved spacing policy is considered to improve road capacity.²⁰ Note that the above DMPC schemes omit inter-vehicle spacing constraints. The inter-vehicle spacing constraints can help to avoid collisions. 18 A DMPC strategy is proposed for a platoon consisting of heterogeneous vehicles to guarantee recursive feasibility and asymptotic stability. Only state penalties are considered in the cost function which may cause serious deceleration/acceleration, resulting in uncomfortable ride for passengers.

Except for the longitudinal movement of vehicles, there is a need of lateral control when driving on curved road. Various methods have been studied for lateral control of a single-vehicle, for example, a nested PID steering control scheme is proposed to achieve path following. Model predictive control (MPC) approach is adopted to design a lateral controller to achieve path following. Robust tube-based MPC method is used to realize path tracking which considers both lateral error and orientation error. A robust sliding model control approach is presented to follow the target path and avoid a large lateral acceleration. Furthermore, an adaptive robust control method is developed to achieve trajectory tracking where parameter perturbations are taken into account.

In recent years, researchers have also paid attention to longitudinal and lateral control of vehicle platoons. A centralized Laguerre-based model predictive controller is designed for longitudinal control of vehicle platoons, and a decentralized tube-based MPC approach is adopted for lateral control to track the reference path where uncertainty of the model and road including bump are considered. A robust approach is developed to ensure the string stability of the vehicle platoon and to achieve path following where communication delays and disturbances are considered. Nevertheless, the aforementioned studies used the decoupled longitudinal and lateral vehicle dynamics. The decoupled dynamics only ensures that the vehicle platoons travel at low speeds on roads with low curvatures.

Therefore, a linear parameter varying (LPV) lateral model is established, which takes into account changing parameters, such as the vehicle longitudinal velocity and yaw rate. The LPV concept is introduced to design a lateral controller which can deal with parametric changes.²⁹ An LPV-based H_{∞} control is introduced for single-vehicles to handle the path tracking problem.³⁰ A linear feedforward and feedback control framework is adopted to ensure longitudinal string stability of platoons, and a linear time varying MPC is proposed to guarantee lane keeping. Note that the interaction between the longitudinal and lateral dynamics is incorporated in the prediction model.³¹ A robust longitudinal control strategy and an LPV lane-keeping control method are proposed for a platoon driving on curved roads.³² However, in these methods, a static longitudinal controller is designed and the lateral position error constraint is ignored in lateral controller, the loss of this constraint may cause the vehicle to leave the road and collide with a vehicle in an adjacent lane. In this paper, a DMPC scheme is proposed for longitudinal control, and the influence of longitudinal velocity and lateral position error constraint are considered in lateral controller to track the reference path.

The above references are listed in Table 1. Most of the existing works on vehicle platoon focus on longitudinal control. Considering the implementation of vehicle platoons, in this paper, an integrated longitudinal and lateral control scheme for vehicle platoons is presented, where lateral controller is designed which considers the changes of longitudinal velocity, and to ensure that the vehicle platoons travel on curved roads at high speeds. Distributed predictive control with terminal inequality constraints is used as the longitudinal controller, and both the recursive feasibility of optimization problem and the asymptotic consensus of vehicle platoons are analyzed. The performance of longitudinal tracking and lane keeping of the vehicle platoon is verified by the joint simulation based on MATLAB/ Simulink and TruckSim. The contributions of this paper are summarized below:

- (1) A DMPC algorithm is presented for the longitudinal control of platoons, where a terminal inequality constraint is imposed to guarantee that recursive feasibility of the involved optimization problem and the asymptotic consensus of the platoon.
- (2) A linear feedforward and feedback control scheme is proposed to track the reference path regardless of longitudinal velocity variations and to satisfy the lateral error constraint.

The rest of this paper is organized as follows. Section "Problem setup" introduces the longitudinal dynamics, the LPV lateral model of a platoon, and the control objective. Both a DMPC algorithm for longitudinal control and a feedforward and feedback control strategy for lateral control are proposed in Section

Table 1. Control method of vehicle platoon.

Control strategy	Related works	Control strategy and main characteristic	Knowledge gap
Longitudinal control	13–15	DMPC: Multi-objective optimization to explicitly handle constraints	Lateral control must be considered to implement lane changing, platoons merging, curved driving, etc.
	3,16,17	DMPC with terminal equality constraint: Consensus of Platoon	merging, curved driving, etc.
	18–20	DMPC with terminal inequality constraint: Recursive feasibility of optimization problem and consensus of Platoon	
Longitudinal and lateral control	26, 27	Longitudinal and lateral decoupled dynamics are used to design controllers	Considering the coupled dynamics can ensure that the vehicle platoons travel on curved roads at high speeds. ²⁸
	31, 32	The influence of longitudinal state is considered in lateral controller and a static longitudinal controller is designed	(1) Model predictive control can explicitly handle constraints and obtain current control action by solving an optimal control problem. (2) Considering longitudinal inter-vehicle spacing constraints can avoid collisions. (3) Considering lateral position error constraint can prevent the vehicle from leaving the lane.

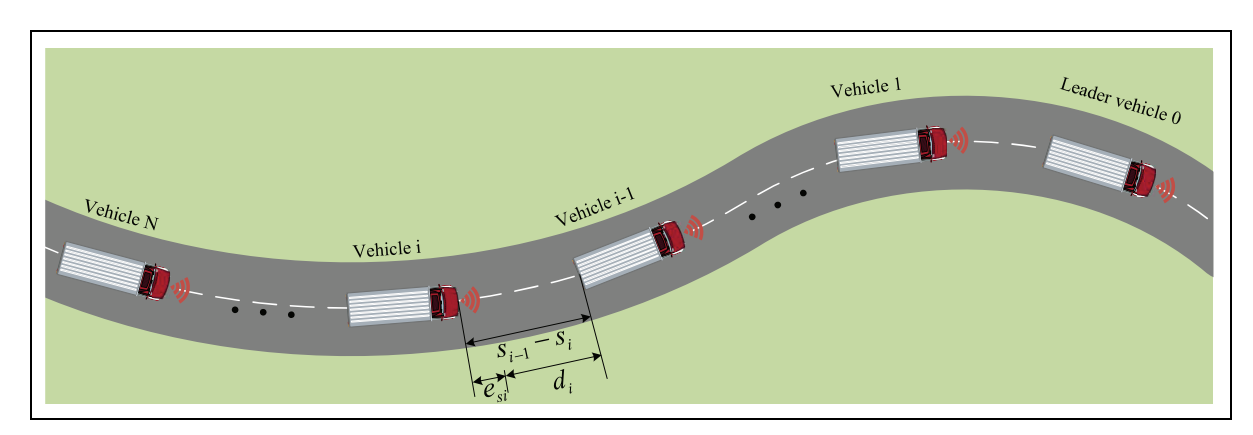


Figure 1. A vehicle platoon drives on a cured road.

"Controller design." Section "Simulation results" shows the joint simulation experiments conducted by MATLAB/Simulink and TruckSim. Section "Conclusions" is the conclusions.

Notation: In this paper, \mathbb{R} represents the set consisting of all real numbers, $\mathbb{R}^{b \times d}$ is the set of $b \times d$ -dimensional real matrices. The notation $\|z\|$ denotes the 2-norm of a vector z. Given a matrix M, $\|z\|_M = z^T M x$ denotes the weighted Euclidean norm. The term z(j|k) represents the predicted value of a variable z at j steps ahead from time k, and the term diag $(g_1, g_2, ..., g_n)$ represents a block-diagonal matrix with elements $g_1, g_2, ..., g_n$ on the main diagonal and zeros in the rest, I_n represents an n-dimensional identity matrix.

Problem setup

As illustrated in Figure 1, a platoon comprising N+1 vehicles is traveling on a curved road. The leading

vehicle of the platoon is numbered 0 and the following vehicles are numbered from 1 to N. Each following vehicle is required to keep a preset distance with neighboring vehicles, and the constant spacing policy is adopted as the desired spacing.

Predecessor-leader following communication topology is adopted, where the following vehicle i only receives information from the leading vehicle 0 and the front vehicle i-1, that is, vehicle's information is only transmitted from upstream to downstream.

The section presents a longitudinal dynamics, and a lateral dynamics in which the longitudinal velocity is treated as a time-varying parameter.

The required symbols for the vehicle platoon system are shown in Table 2.

Longitudinal dynamics

The longitudinal dynamic model of *i*th vehicle in a platoon is defined by a third-order nonlinear model⁹:

Table 2. Symbols for vehicle platoon system.

Symbol	Description
si	Position of the <i>i</i> th vehicle
$\mathbf{v}_{i}^{\mathbf{x}}$	Longitudinal velocity of the ith vehicle
\mathbf{v}_{i}^{x} \mathbf{v}_{i}^{y}	Lateral velocity of the ith vehicle
a_i	Longitudinal acceleration of the <i>i</i> th vehicle The yaw rate
$egin{array}{l} \dot{arphi}_i \ \mathbf{e}^{s}_i \ \mathbf{e}^{v}_i \ \mathbf{v}^{y}_i \ \mathbf{I}^{z}_i \end{array}$	The position error of the <i>i</i> th vehicle
e,v	The velocity error of the ith vehicle
$\mathbf{v}_{i}^{\dot{y}}$	Lateral velocity of the ith vehicle
I ^ź	The inertia moment around the z-axis
$I_{f,i}$	The distances from the front axle to the center of mass
$I_{r,i}$	The distances from the rear axle to the center of mass
F ^f	The lateral forces imposed on the front tires
F _i ' C ^f	The lateral forces imposed on the rear tires The cornering stiffness of the front tires
F [†] _i F' _i C' _i C' _i δ _i	The cornering stiffness of the rear tires The steering angle of front tires The road curvature

$$\begin{cases} \dot{s}_{i} = v_{i}^{x} \\ \dot{v}_{i}^{x} = \frac{1}{m_{i}} \left(\frac{\eta_{i}}{R_{i}} T_{i} - \frac{1}{2} C_{i}^{d} A_{i} \rho_{i} (v_{i}^{x})^{2} - m_{i} g f_{i} \right) \\ \dot{T}_{i} = -\kappa_{i}^{-1} T_{i} + \kappa_{i}^{-1} T_{i}^{des} \end{cases}$$
(1)

where s_i , v_i^x , and T_i are position, longitudinal velocity, and actual driving/braking torque. The term of η_i denotes the mechanical efficiency of driveline, m_i denotes the mass, R_i represents the rolling radius of the tires, A_i denotes windward area, ρ_i represents the air density, f_i denotes the coefficient of rolling resistance, C_i^d represents aerodynamic drag coefficient, g denotes the gravity constant, κ_i represents the time constant of longitudinal dynamics. The term of T_i^{des} denotes the desired control torque.

Assume that all parameters in (1) are known a priori. Then, the nonlinear feedback control law is adopted as follows:

$$T_i^{des} = \frac{R_i}{\eta_i} \left(m_i u_i + m_i g f_i + \frac{1}{2} C_i^d A_i \rho_i v_i^x (2\kappa_i a_i + v_i^x) \right)$$
(2)

which transforms (1)–(3)

$$\begin{cases}
\dot{s}_i = v_i^x \\
\dot{v}_i^x = a_i \\
\dot{a}_i = -\kappa_i^{-1} a_i + \kappa_i^{-1} u_i^x
\end{cases}$$
(3)

where a_i is the longitudinal acceleration, u_i^x is the control input of (3).³³

The model (3) is discretized by using a sampling time $T_s > 0$

$$\begin{cases} s_i(k+1) = s_i(k) + v_i^x(k)T_s \\ v_i^x(k+1) = v_i^x(k) + a_i(k)T_s \\ a_i(k+1) = (1 - \frac{T_s}{\kappa_i})a_i(k) + \frac{T_s}{\kappa_i}u_i^x(k) \end{cases}$$
(4)

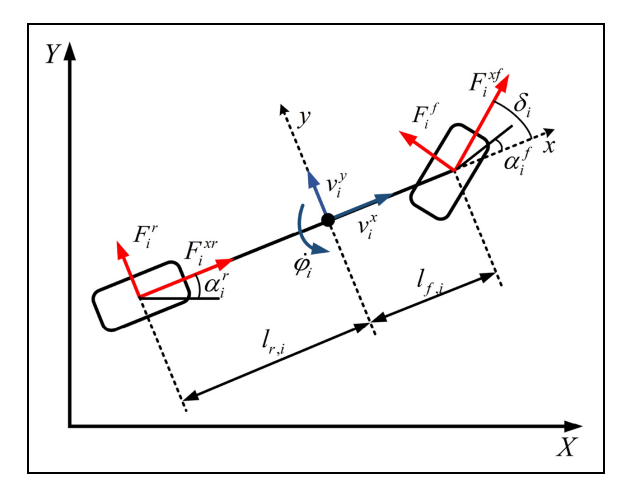


Figure 2. Bicycle model for lateral dynamics of vehicle i.

The position error of the *i*th vehicle is the difference between the desired position and the actual position, which is described by

$$e_i^s(k) = (s_0(k) - d_{i,0}) - s_i(k)$$
(5)

where $d_{i,0} = i \cdot d_0$ is the desired spacing of *i*th vehicle.

Define $e_i^{\nu}(k)$ as the velocity error of the *i*th following vehicle which is the difference between the desired and actual velocity, that is,

$$e_i^{\nu}(k) = v_0^{\nu}(k) - v_i^{\nu}(k) \tag{6}$$

where $v_0^x(k)$ is the velocity of leading vehicle.

Denote $x_i := [e_i^s(k), e_i^v(k), a_i(k)]^T \in \mathbb{R}^{3 \times 1}$. Then, the longitudinal error model of the *i*th following vehicle is

$$x_i(k+1) = A_i^x x_i(k) + B_i^1 u_i(k) + B_i^2 a_0(k)$$
 (7)

with $A_{i}^{x} = \begin{bmatrix} 1 & T_{s} & 0 \\ 0 & 1 & T_{s} \\ 0 & 0 & -\frac{T_{s}}{T_{s}} \end{bmatrix}, B_{i}^{1} = \begin{bmatrix} 0 \\ 0 \\ \frac{T_{s}}{T_{s}} \end{bmatrix}, B_{i}^{2} = \begin{bmatrix} 0 \\ 0 \\ T \end{bmatrix}.$

Concerning system (7), the following lemma is needed to determine the terminal control law, the terminal region, and the terminal penalty of the DMPC.

Lemma 1.³⁴ For system (7) there exits a linear state feedback law $u_i^x = K_i x_i$ such that $A_{K,i} = A_i^x + B_i^1 K_i$ is asymptotically stable.

Furthermore, (i) there exits a unique positive-definite and symmetric matrix P_i such that

$$A_{Ki}^{T} P_{i} A_{K,i} + P_{i} = -Q_{i}^{*} (8)$$

where $Q_i^* = Q_i + K_i^T R_i K_i$, and $A_{K,i} = A_i^x + B_i^1 K_i$. (ii) The neighborhood X_i^N of the origin

$$\mathbb{X}_{i}^{N}(\alpha) := \left\{ x \in \mathbb{R}^{n} | x_{i}^{T} P_{i} x_{i} \leq \alpha \right\}$$

$$\tag{9}$$

is an terminal region for system (7) with $\alpha > 0$.

Then, $K_i x_i$, X_i^N , and $x_i^T P_i x_i$ are named the terminal control law, the terminal region, and the terminal penalty, respectively.

Lateral dynamics

The lateral dynamic model is derived from a simplified two degrees of freedom bicycle model, which is illustrated in Figure 2. The nonlinear lateral dynamic model is described as follows.³⁵

$$\begin{cases}
 m_i \dot{v}_i^y + m_i v_i^x \dot{\phi}_i = F_i^f + F_i^r \\
 F_i^r \ddot{\phi}_i = I_{f,i} F_i^f - I_{r,i} F_i^{yr}
\end{cases}$$
(10)

where v_i^y denotes the lateral velocity of *i*th vehicle, $\dot{\varphi}_i$ denotes the yaw rate, I_i^z denotes the inertia moment around the z-axis, m_i represents the mass. The terms of $l_{f,i}$ and $l_{r,i}$ denote the distances from the front and rear axles to the center of mass, respectively. The terms of F_i^f and F_i^r represent the lateral forces imposed on the front and rear tires, respectively.

Suppose that the front and rear tires work in their linear region. Then, the tire forces F_i^f and F_i^r are calculated using the small angle approximation method, that is,

$$\begin{cases}
F_i^f = C_i^f \left(\delta_i - \frac{v_i^y + l_{f,i}\phi_i}{v_i^y} \right) \\
F_i^r = C_i^r \left(\frac{l_{f,i}\phi_i - v_i^y}{v_i^y} \right)
\end{cases}$$
(11)

where C_i^f and C_i^r represent the cornering stiffness of the front and rear tires, respectively, δ_i represents the steering angle of front tires.

The lateral dynamic model of vehicle i can be rewritten by combining (10) and (11) as

$$\begin{cases} \dot{v}_{i}^{y} = -v_{i}^{x}\dot{\phi}_{i} + \frac{1}{m_{i}} \left(-\frac{\left(C_{i}^{f} + C_{i}^{r}\right)v_{i}^{y}}{v_{i}^{x}} - \frac{\left(C_{i}^{f}l_{f,i} - C_{i}^{r}l_{r,i}\right)\dot{\phi}_{i}}{v_{i}^{x}} + C_{i}^{f}\delta_{i} \right) \\ \ddot{\phi}_{i} = \frac{1}{I_{i}^{r}} \left(-\frac{\left(C_{i}^{f}l_{f,i} - C_{i}^{r}l_{r,i}\right)v_{i}^{y}}{v_{i}^{x}} - \frac{\left(C_{i}^{f}l_{f,i}^{2} + C_{i}^{r}l_{r,i}^{2}\right)\dot{\phi}_{i}}{v_{i}^{x}} + C_{i}^{f}l_{f,i}\delta_{i} \right) \end{cases}$$

$$(12)$$

Generally speaking, lateral control of a vehicle platoon expects the vehicles in the platoon to move along the centerline of the road, that is, the actual driving path is consistent with the reference path and the error between them should be close to zero. Therefore, the lateral error dynamic model is introduced as illustrated in Figure 3.

The lateral position error between the center of mass of the *i*th vehicle and the centerline of a lane is denoted by e_i^{ν} . Then the rate of the lateral position error is

$$\dot{e}_i^y = v_i^y + v_i^x e_i^{\varphi} \tag{13}$$

Furthermore, \ddot{e}_{i}^{y} is

$$\ddot{e}_i^y = \dot{v}_i^y + v_i^x \dot{e}_i^{\varphi} \tag{14}$$

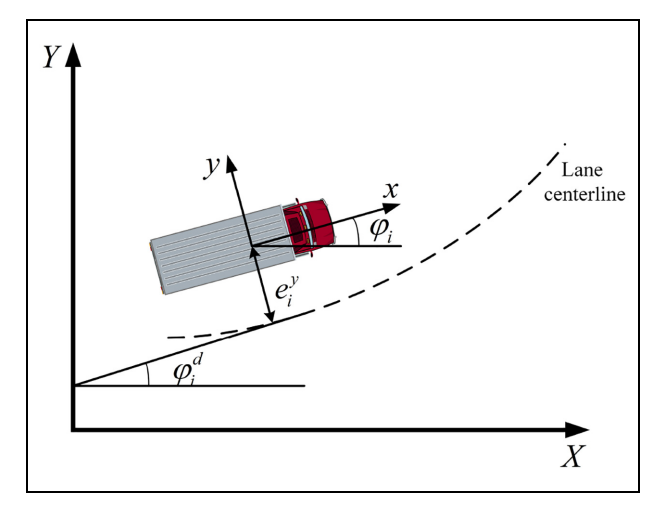


Figure 3. The structure of lateral error dynamic model.

The heading error of *i*th vehicle with respect to the centerline of a lane is defined as

$$e_i^{\varphi} = \varphi_i - \varphi_i^d \tag{15}$$

where φ_i is the heading angle of *i*th vehicle, φ_i^d denotes the orientation angle of a lane centerline.

Furthermore, the rate of the heading error is as follows

$$\dot{e}_i^{\varphi} = \dot{\varphi}_i - \dot{\varphi}_i^d \tag{16}$$

where $\dot{\varphi}_i^d$ denotes the desired yaw rate, and

$$\dot{\varphi}_i^d = v_i^x c_i \tag{17}$$

where c_i is the road curvature.

Substituting (12) into (14) and (16) yields

$$m_{i}\ddot{e}_{i}^{v} = \dot{e}_{i}^{v} \left(-\frac{C_{i}^{f}}{v_{i}^{x}} - \frac{C_{i}^{r}}{v_{i}^{x}} \right) + e_{i}^{\varphi} \left(C_{i}^{f} + C_{i}^{r} \right)$$

$$+ \dot{e}_{i}^{\varphi} \left(-\frac{C_{i}^{f} l_{f,i}}{v_{i}^{x}} + \frac{C_{i}^{r} l_{r,i}}{v_{i}^{x}} \right)$$

$$+ \dot{\varphi}_{i}^{d} \left(-\frac{C_{i}^{f} l_{f,i}}{v_{i}^{x}} + \frac{C_{i}^{r} l_{r,i}}{v_{i}^{x}} - m_{i} v_{i}^{x} \right) + C_{i}^{f} \delta_{i}$$

$$(18)$$

and

$$I_{i}^{z}\ddot{e}_{\varphi,i} = \dot{e}_{i}^{y}\left(-\frac{C_{i}^{f}I_{f,i}}{v_{i}^{x}} + \frac{C_{i}^{r}I_{r,i}}{v_{i}^{x}}\right) + e_{i}^{\varphi}\left(C_{i}^{f}I_{f,i} - C_{i}^{r}I_{r,i}\right) + \dot{e}_{i}^{\varphi}\left(-\frac{C_{i}^{f}I_{f,i}^{2}}{v_{i}^{x}} - \frac{C_{i}^{r}I_{r,i}^{2}}{v_{i}^{x}}\right) + \dot{\varphi}_{i}^{d}\left(-\frac{C_{i}^{f}I_{f,i}^{2}}{v_{i}^{x}} - \frac{C_{i}^{r}I_{r,i}^{2}}{v_{i}^{x}}\right) + C_{i}^{f}I_{f,i}\delta_{i}$$

$$(19)$$

Define the state as $z_i = \begin{bmatrix} e_i^y & \dot{e}_i^y & e_i^\phi & \dot{e}_i^\phi \end{bmatrix}$ and control input as $u_i^y = \delta_i$. Choosing v_i^x as the varying parameter, the LPV lateral error dynamics state space model is therefore given by

$$\dot{z}_i = A_i^y(v_i^x)z_i + B_i^y u_i^y + E_i \dot{\varphi}_i^d \tag{20}$$

where

$$\begin{split} &A_{i}^{y}(v_{i}^{x}) = \\ &\begin{bmatrix} 0 & 1 & 0 & 0 \\ 0 & -\frac{(C_{i}^{f} + C_{i}^{r})}{m_{i}v_{i}^{x}} & \frac{(C_{i}^{f} + C_{i}^{r})}{m_{i}} & -\frac{(C_{i}^{f}l_{f,i} - C_{i}^{r}l_{r,i})}{m_{i}v_{i}^{x}} \\ 0 & 0 & 0 & 1 \\ 0 & -\frac{(C_{i}^{f}l_{f,i} - C_{i}^{r}l_{r,i})}{I_{z,i}v_{i}^{x}} & -\frac{(C_{i}^{f}l_{f,i} - C_{i}^{r}l_{r,i})}{I_{z,i}} & -\frac{(C_{i}^{f}l_{f,i} - C_{i}^{r}l_{r,i})}{I_{z,i}v_{i}^{x}} \end{bmatrix} \\ &B_{i}^{y} = \begin{bmatrix} 0 \\ \frac{C_{i}^{f}}{m_{i}} \\ 0 \\ \frac{C_{i}^{f}l_{f,i}}{I_{z,i}} \end{bmatrix}, E_{i} = \begin{bmatrix} 0 \\ \frac{C_{i}^{f} + C_{i}^{r}}{m_{i}v_{i}^{x}} - v_{i}^{x} \\ 0 \\ -\frac{C_{i}^{f}l_{f,i} + C_{i}^{r}l_{r,i}^{r}}{I_{z,i}v_{i}^{x}} \end{bmatrix} \end{split}$$

Obviously, the matrix $A_i^v(v_i^x)$ depends on the varying parameter $v_i^x \in \begin{bmatrix} v_{\min,i}^x & v_{\max,i}^x \end{bmatrix}$, where $v_{\min,i}^x$ and $v_{\max,i}^x$ denote the allowed minimum and maximum velocity. Denote the matrices $A_{\min,i}^y$ and $A_{\max,i}^y$ as

$$\begin{split} A_{\min,i}^{y} &= A_i^{y}(v_i^{x})|_{v_i^{x} = v_{\max,i}^{x}} \\ A_{\max,i}^{y} &= A_i^{y}(v_i^{x})|_{v_i^{x} = v_{\min,i}^{x}} \end{split}$$

The matrix $A_i^y(v_i^x)$ belongs to a polytopic matrix Σ , that is,

$$\Sigma := Co\left\{A_{\min,i}^{y}, A_{\max,i}^{y}\right\} \tag{21}$$

where $Co\{.\}$ is a convex hull of matrices.

Control objective

The overall control objective of a vehicle platoon is that each following vehicle tracks the velocity of the leading vehicle and follows the centerline of a lane while maintaining a designed spacing with neighboring vehicles. It consists of longitudinal and lateral control objectives.

Longitudinal control objective. The control objectives of longitudinal driving are to track the longitudinal velocity of the leading vehicle and eliminate the position error between the desired and actual positions of vehicle *i*, that is

$$\begin{cases} minimize \left\| e_i^s(t) \right\|_2^2 = 0\\ minimize \left\| e_i^v(t) \right\|_2^2 = 0 \end{cases}$$
(22)

To ensure the safe driving, each vehicle *i* must satisfy the following constraints:

$$e_i^s(t) \in \left[e_{\min}^s, e_{\max}^s \right] \tag{23a}$$

$$e_i^{\mathbf{v}}(t) \in \left[e_{\min}^{\mathbf{v}}, e_{\max}^{\mathbf{v}} \right] \tag{23b}$$

where e_{\min}^s and e_{\max}^s represent the tolerable minimum and maximum value of position errors, e_{\min}^v and e_{\max}^v represent the tolerable minimum and maximum value of velocity errors, and $0 \in \left[e_{\min}^s, e_{\max}^s\right]$ and $0 \in \left[e_{\min}^v, e_{\max}^v\right]$.

Lateral control objective. The control objective for the lateral performance of the platoon is to follow the centerline of the road, as demonstrated by the lateral position error and the heading error of each vehicle *i* are as close to zero as possible

$$\begin{cases}
minimize \|e_i^{\varphi}(t)\|_2^2 = 0 \\
minimize \|e_i^{y}(t)\|_2^2 = 0
\end{cases}$$
(24)

To ensure that all vehicles in the platoon drive within the road boundary, the following constraint must be satisfied:

$$e_i^{y}(t) \in \left[e_{\min}^{y}, e_{\max}^{y} \right] \tag{25}$$

where e_{\min}^{ν} and e_{\max}^{ν} denote the tolerable minimum and maximum values of lateral position errors.

Controller design

In this section, an integrated longitudinal and lateral control framework is employed which is illustrated in Figure 4.

For longitudinal control, a distributed model predictive controller is designed, where terminal inequality constraint is introduced to guarantee the asymptotic consensus of the vehicle platoon.

For lateral control, a feedforward combined with a robust feedback control strategy is presented. The robust feedback control law is determined by solving linear matrix inequalities, which guarantees that the road constraint (25) is satisfied, whatever the longitudinal velocity changes. Furthermore, to eliminate the lateral position error, a feedforward control law is designed.

Longitudinal distributed model predictive controller

DMPC divides a global optimization problem into N independent local optimization problems. For following vehicle i, a local individual optimization problem

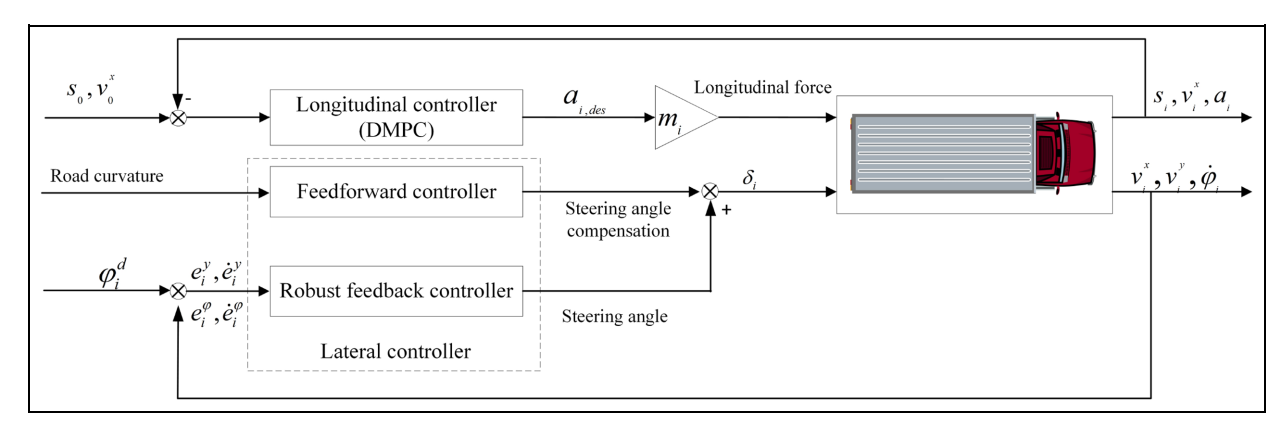


Figure 4. The integrated control framework of the vehicle i.

requires only the position and velocity of the vehicles 0 and i - 1.

Define R_H as the predictive horizon, and define $U_i^x(k) = \{u_i^x(0|k), u_i^x(1|k), \dots, u_i^x(R_H - 1|k)\}$ as the control sequence for vehicle i.

Assumption 1. The leading vehicles in a platoon is traveling at a given steady speed, that is, $a_0 = 0$.

The open-loop optimization problem of following vehicle i at time k is

Problem 1

$$\underset{U^{N}(k)}{\text{minimize}} L_{i}(x_{i}(k), u_{i}^{x}(k)) \tag{26a}$$

Subject to

$$x_i(k+1) = A_i^x x_i(k) + B_i^1 u_i^x(k)$$
 (26b)

$$x_i(0|k) = x_i(k) \tag{26c}$$

$$e_i^s(j|k) \in \left[e_{\min}^s, e_{\max}^s\right] \tag{26d}$$

$$e_i^{\nu}(j|k) \in \left[e_{\min}^{\nu}, e_{\max}^{\nu} \right] \tag{26e}$$

$$a_i(j|k) \in [a_{\min}, a_{\max}] \tag{26f}$$

$$x_i(R_H|k) \in \mathbb{X}_i^N(\alpha) \tag{26g}$$

where the cost function is

$$L_{i}(x_{i}(k), u_{i}^{x}(k)) = \sum_{j=0}^{R_{H}-1} l_{i}(x_{i}(j|k), u_{i}^{x}(j|k)) + F(x_{i}(R_{H}|k))$$

The stage cost function is

$$l_i(x_i(j|k), u_i^x(j|k)) = \|x_i(j|k)\|_{O_i}^2 + \|u_i^x(j|k)\|_{R_i}^2$$
 (27)

where $Q_i > 0$ and $R_i > 0$ are weighting matrices.

The terminal penalty matrix P_i and the terminal region $\mathbb{X}_i^N(\alpha)$ are solved offline by Lemma 1. The terminal cost is $F(x_i) = x_i^T P_i x_i$. The terminal inequality constraint (26g) enforces the terminal states to the terminal set.

At time k > 0, each vehicle *i* receives state information of the leading vehicle. Then the state $x_i(k)$ is used to solve Problem 1 to yield the optimal control sequence

$$U_i^{x^*}(k) = \left\{ u_i^{x^*}(0|k), u_i^{x^*}(1|k), \dots, u_i^{x^*}(R_H - 1|k) \right\}$$

and the corresponding optimal state trajectory is calculated as follows

$$x_i^*(j+1|k) = A_i^x x_i^*(j|k) + B_i^1 u_i^{x^*}(j|k)$$
 (28)

Define a feasible control sequence of the system (7) at the next sampling time k + 1 as follows

$$u_i^{x}(j|k+1) = \begin{cases} u_i^{x^*}(j+1|k), & j=0,1,...,R_H-1\\ K_i x_i^*(j|k), & j=R_H \end{cases}$$
(29)

The corresponding state trajectory is calculated by

$$x_{i}(j|k+1) = \begin{cases} x_{i}^{*}(j+1|k), & j=0,...,R_{H}-1\\ A_{i}^{x}x_{i}^{*}(j|k) + B_{i}^{1}\hat{u}_{i}^{x}(j|k+1) & j=R_{H} \end{cases}$$
(30)

The following theorem shows that Problem 1 is recursive feasibility, and the platoon is asymptotic consensus.

Theorem 2. Suppose that the terminal penalty matrix P_i and terminal region $\mathbb{X}_i^N(\alpha)$ have been determined by Lemma 1. For following vehicle i, if Problem 1 is feasible at the initial time k = 0 with the state $x_i(0)$ and the control input $u_i^X(0)$, then

- (1) Problem 1 is recursive feasibility.
- (2) System (7) is asymptotically stable, that is, $x_i(k) \to 0$ as $k \to \infty$. Thus, the platoon is asymptotic consensus.

Proof: (1) Suppose that, at time instant k, Problem 1 is feasible with the state $x_i(k)$ and control input $u_i^x(k)$. The optimal control sequence $U_i^{x^*}(k)$ is obtained by solving Problem 1, and the corresponding optimal state trajectory $x_i^*(j|k)$ ($j=0,1,...,R_H$) is calculated which satisfies the constraints (26c)–(26f). Besides, the optimal terminal error state enters the terminal region, that is, $x_i^*(R_H|k) \in \mathbb{X}_i^N(\alpha)$.

At next time instant k + 1, the initial state of the system (7) is $x_i(k + 1) = x_i^*(1|k)$. That is, the updated initial condition (26c) is $x_i(0|k + 1) = x_i(k + 1)$. Therefore, the following control function can be preselected:

$$\hat{u}_{i}^{x}(j|k+1) = \begin{cases} u_{i}^{x^{*}}(j+1|k), & j=0,1,...,R_{H}-1, \\ K_{i}x_{i}(j|k+1), & j=R_{H} \end{cases}$$
(31)

The equation (31) consists of two parts. The first part is at $j = 0, 1, ..., R_H - 1$, the corresponding state trajectories are $x_i(j|k+1) = x_i^*(j+1|k)$ which satisfies the constraints (26c)–(26f) and the terminal state enters terminal region, that is, $x_i(R_H - 1|k+1) \in \mathbb{X}_i^N(\alpha)$. The second part is at $j = R_H$, the corresponding state trajectories starting at $x_i(j|k+1) \in \mathbb{X}_i^N(\alpha)$ are always in $\mathbb{X}_i^N(\alpha)$ due to $\mathbb{X}_i^N(\alpha)$ is an invariant set, cf. Lemma 1.

(2) At time instant k, the state of the system (7) is $x_i(k)$ and a feasible control sequence is $U_i^x(k)$. Solving the optimal Problem 1 yields an optimal control sequence $U_i^{x^*}(k)$ and a corresponding optimal error state trajectory $x_i^*(j|k)$ ($j = 0, 1, ..., R_H$). Thus, the optimal cost function of Problem 1 at time instant k is

$$L_i^*(k) = \sum_{j=0}^{R_H - 1} l_i(x_i^*(j|k), u_i^{x^*}(j|k)) + F(x_i^*(R_H|k))$$
 (32)

At time instant k + 1, the cost function is

$$L_{i}(k+1) = \sum_{j=0}^{R_{H}-1} l_{i}(x_{i}(j|k+1), u_{i}^{x}(j|k+1)) + F(x_{i}(R_{H}|k+1))$$
(33)

Combine (29), (30) and (33) to obtain

$$L_{i}(k+1) = \sum_{j=1}^{R_{H}-1} l_{i}(x_{i}^{*}(j|k), u_{i}^{x^{*}}(j|k))$$

$$+ F(x_{i}(R_{H}|k+1)) + l_{i}(x_{i}(R_{H}-1|k+1),$$

$$u_{i}^{x}(k+R_{H}-1|k+1))$$

$$= L_{i}^{*}(k) - l_{i}(x_{i}^{*}(0|k), u_{i}^{x^{*}}(0|k))$$

$$- F(x_{i}^{*}(R_{H}|k)) + l_{i}(x_{i}(R_{H}-1|k+1),$$

$$u_{i}^{x}(R_{H}-1|k+1))$$

$$+ F(x_{i}(R_{H}|k+1))$$
(34)

Due to $x_i(R_H - 1|k+1) = x_i^*(R_H|k)$ and $x_i^*(R_H|k) \in \mathbb{X}_i^N(\alpha)$, one has

$$l_{i}(x_{i}(R_{H}|k+1), u_{i}^{x}(R_{H}|k+1)) + F(x_{i}(R_{H}|k+1) - F(x_{i}^{*}(R_{H}|k)) \leq 0$$
(35)

In terms of (34) and (35), it yields:

$$L_i(k+1) \le L_i^*(k) - l_i(x_i^*(0|k), u_i^{x^*}(0|k))$$
 (36)

which implies that

$$L_i^*(k+1) - L_i^*(k) \leqslant -l_i(x_i^*(0|k), u_i^{x^*}(0|k)) \leqslant 0$$
 (37)

where the fact of $L_i^*(k+1) \leq L_i(k+1)$ is used. Thus,

$$L_i^*(k+1) \leqslant L_i^*(k) \tag{38}$$

and $x_i(k) \to 0$ as $k \to \infty$, that is, the platoon is asymptotic consensus.

Remark 1. Due to the inherent robustness of linear MPC, 36,37 recursive feasibility and asymptotic stability can be guaranteed while $a_0(j|k)$, $j \in [k, k + R_H]$ is small.

Lateral controller

In this subsection, a feedforward and feedback control scheme is used that consists of (1) a robust feedback controller minimizes the current heading error and lateral position error regardless of longitudinal velocity variations; (2) a feedforward controller eliminates the lateral position error when front wheel steering angle is optimized by the robust feedback controller.

Feedback controller. Suppose that the vehicle is traveling on a straight road (i.e. the road curvature $c_i = 0$, the desired yaw rate $\dot{\varphi}_i^d = 0$), the system (20) can be rewritten as follows

$$\dot{\bar{z}}_i = A_i^y(v_i^x)\bar{z}_i + B_i^y u_i^y \tag{39}$$

As for the system (39), we define the following quadratic cost index

$$J_{y,i} = \int_0^\infty [\bar{z}_i E_i \bar{z}_i + (u_i^y)^T H_i u_i^y] dt$$
 (40)

where E_i and H_i are given positive-definite symmetric matrices

After that, a feedback control law must be designed which minimizes the cost function (40) and ensures that the closed-loop system of the LPV system (39) is asymptotically stable whatever the longitudinal velocity changes. The robust feedback control law is

$$u_i^{y} = G_i \bar{z}_i \tag{41}$$

where $G_i = \begin{bmatrix} g_{1,i} & g_{2,i} & g_{3,i} & g_{4,i} \end{bmatrix}$ is the gain matrix.

The following theorem is presented to obtain the state feedback control law (41) for the LPV system (39).

Theorem 3. Suppose that there exits a positive scalar ε , a matrix G_i , and a symmetric positive-definite matrix M_i such that the following linear matrix inequalities are satisfied

$$\begin{bmatrix} \Omega_i & X_i & W_i \\ * & -E_i^{-1} & 0 \\ * & * & -H_i^{-1} \end{bmatrix} < 0$$
 (42)

$$\begin{bmatrix} \frac{1}{\varepsilon} (e_{\max}^{y})^{2} & e_{j}^{T} X_{i} \\ * & X_{i} \end{bmatrix} \ge 0 \tag{43}$$

where e_j is the jth standard vector basis, $X_i = M_i^{-1}$, $W_i = G_i M_i^{-1}$ and

$$\Omega_{i} = A_{i}^{y}(v_{i}^{x})X_{i} + B_{i}^{y}W_{i} + (A_{i}^{y}(v_{i}^{x})X_{i} + B_{i}^{y}W_{i})^{T}$$
 (44)

Furthermore, if (42) and (43) admit a feasible solution W_i^* , $X_i^* > 0$, then the state feedback control $u_i^y = W_i^* X_i^* - 1z_i$ ensures that the closed-loop system of the LPV system (39) is asymptotically stable whatever the longitudinal velocity changes.

The proof of the Theorem 3 is divided into two steps. First, the linear matrix inequality (42) for performance of system is proved. Then, the linear matrix inequality of constraint satisfaction (43) is proved.

Proof: (1) Let $u_i^v = G_i \overline{z}_i$ in (39), then the closed-loop system is:

$$\dot{\bar{z}}_i = (A_i^y + B_i^y G_i) \bar{z}_i \tag{45}$$

Define $V(\bar{z}_i) = \bar{z}_i^T M_i \bar{z}_i$ as a candidate Lyapunov function. The time derivative of $V(\bar{z}_i)$ is obtained at any trajectory of the closed-loop system (45), that is,

$$\dot{V}(\bar{z}_i) = \bar{z}_i^T \{ M_i [A_i^y + B_i^y G_i] + [A_i^y + B_i^y G_i]^T M_i \} \bar{z}_i \quad (46)$$

Then, the closed-loop system is asymptotically stable if there exits $M_i > 0$ such that

$$\dot{V}(\bar{z}_i) < -\bar{z}_i^T (E_i + G_i^T H_i G_i) \bar{z}_i < 0 \tag{47}$$

Equation (47) is equivalent to

$$E_{i} + G_{i}^{T} H_{i} G_{i} + M_{i} [A_{i}^{y} + B_{i}^{y} G_{i}] + [A_{i}^{y} + B_{i}^{y} G_{i}]^{T} M_{i} < 0$$

$$(48)$$

It follows from the Schur complement that (48) is equivalent to the following

$$\begin{bmatrix} \bar{\Omega}_i & I & G_i^T \\ * & -E_i^{-1} & 0 \\ * & * & -H_i^{-1} \end{bmatrix} < 0$$
 (49)

where $\bar{\Omega}_i = M_i [A_i^y + B_i^y G_i] + [A_i^y + B_i^y G_i]^T M_i$.

Pre- and post-multiply both sides of the inequality (49) by $diag(M_i^{-1}, I, I)$, then

$$\begin{bmatrix} \tilde{\Omega}_i & M_i^{-1} & G_i M_i^{-1} \\ * & -E_i^{-1} & 0 \\ * & * & -H_i^{-1} \end{bmatrix} < 0$$
 (50)

where

$$\tilde{\Omega}_{i} = A_{i}^{y}(v_{i}^{x})M_{i}^{-1} + B_{i}^{y}G_{i}M_{i}^{-1} + (A_{i}^{y}(v_{i}^{x})M_{i}^{-1} + B_{i}^{y}G_{i}M_{i}^{-1})^{T}$$

Denote $X_i = M_i^{-1}$, $W_i = G_i M_i^{-1}$. Then, (50) is equivalent to inequality (42).

(2) State constraint (25) implies that $(e_i^y)^2 \le (e_{\max}^y)^2$. In accordance with $e_i^y = e_i^T \bar{z}_i$, then

$$\bar{z}_i^T e_j e_j^T \bar{z}_i \leqslant (e_{\text{max}}^{\nu})^2 \tag{51}$$

A sufficient condition of (51) is

$$\bar{z}_i^T \frac{e_j e_j^T}{(e_{\max}^y)^2} \bar{z}_i \leqslant \bar{z}_i^T \frac{M_i}{\varepsilon} \bar{z}_i$$
 (52)

that is,

$$\frac{M_i}{\varepsilon} - \frac{e_j e_j^T}{\left(e_{\text{max}}^V\right)^2} \ge 0 \tag{53}$$

By Schur complement, (53) is equivalent to

$$\begin{bmatrix} \frac{1}{\varepsilon} (e_{\text{max}}^{y})^{2} & e_{j}^{T} \\ * & M_{i} \end{bmatrix} \ge 0 \tag{54}$$

By pre- and post-multiplying $diag(I, M_i^{-1})$, the inequality (49) can be represented as

$$\begin{bmatrix} \frac{1}{\varepsilon} (e_{\text{max}}^{y})^{2} & e_{j}^{T} M_{i}^{-1} \\ * & M_{i}^{-1} \end{bmatrix} \geqslant 0$$
 (55)

The inequality (43) is obtained by substituting $X_i = M_i^{-1}$, $W_i = G_i M_i^{-1}$ into the inequality (55).

Feedforward controller. When the vehicle is traveling on a cured road (i.e. the road curvature $c_i \neq 0$, the desired yaw rate $\dot{\varphi}_i^d \neq 0$), the lateral dynamics is (20). If the control law is (41), then the closed-loop system of (20) is

$$\dot{z}_i = [A_i^y(v_i^x) + B_i^y G_i] z_i + E_i \dot{\varphi}_i^d$$
 (56)

The equation (56) implies that even though $[A_i^y(v_i^x) - B_i^yG_i]$ is asymptotically stable, but the lateral error is impacted by the road curvature c_i . Note that the relationship between the desired yaw rate $\dot{\phi}_i^d$ and the road curvature c_i is $\dot{\phi}_i^d = v_i^x c_i$. To eliminate the influence of the road curvature c_i , a feedforward controller is designed, and the control law for system (20) is

$$u_i^{y} = G_i z_i + \delta_{f,i} \tag{57}$$

Combine (20) and (57), the closed-loop system is

$$\dot{z}_i = [A_i^y(v_i^x) + B_i^y G_i] z_i + B_i^y \delta_{f,i} + E_i \dot{\varphi}_i^d$$
 (58)

Take the Laplace transform of (58) with zero initial conditions, one obtains

$$Z_{i}(s) = [sI - A_{i}^{y}(v_{i}^{x}) + B_{i}^{y}G_{i}]^{-1}[B_{i}^{y}L(\delta_{f,i}) + E_{i}L(\dot{\varphi}_{i}^{d})]$$
(59)

where $L(\delta_{f,i})$ and $L(\dot{\varphi}_i^d)$ are Laplace transform of $\delta_{f,i}$ and $\dot{\varphi}_i^d$, respectively.

$$z_{ss,i} = \lim_{t \to \infty} z_i(t)$$
 (i.e. one leading truck and three
$$= \lim_{s \to 0} s Z_i(s)$$

$$= \begin{bmatrix} \frac{\delta_{f,i}}{g_{1,i}} \\ 0 \\ 0 \\ 0 \end{bmatrix} + \begin{bmatrix} -\frac{1}{g_{1,i}} \frac{m_i(v_i^x)^2 c_i}{l_{f,i} + l_{r,i}} \left(\frac{l_{r,i}}{2C_{f,i}} - \frac{l_{f,i}}{2C_i^r} + \frac{l_{f,i}}{2C_i^r} g_{3,i} \right) - \frac{c_i}{g_{1,i}} \left(l_{f,i} + l_{r,i} - l_{r,i} g_{3,i} \right) \\ 0 \\ \frac{c_i}{2C_i^r (l_{f,i} + l_{r,i})} \left(-2C_i^r l_{f,i} l_{r,i} - 2C_i^r l_{r,i}^2 + l_{f,i} m_i(v_i^x)^2 \right) \\ 0 \end{bmatrix}$$

The Final Value Theorem is used to determine the steady state value of the system (58), that is (60). To achieve an offset free steady-state value of the lateral error of the closed-loop system (58), the feedforward term is selected as follows

$$\delta_{f,i} = c_i \left[L_i - g_{3,i} l_{r,i} - \frac{m_i (v_i^x)^2}{L_i} \left(\frac{l_{f,i}}{C_i^r} + \frac{l_{r,i}}{C_{f,i}} g_{3,i} - \frac{l_{r,i}}{C_{f,i}} \right) \right]$$
(61)

where $g_{3,i}$ is the gain coefficient in the first row and third column of the gain matrix G_i , and $L_i = l_{f,i} + l_{r,i}$.

Table 3. Parameters of trucks.

Parameters	Value	Parameters	Value
m _i I _{f,i} I ^z	18,000 kg 3.5 m 130,421.8 kg m ²	Ki I _{r, i}	0.4 1.5 m

Table 4. Penalty matrices.

Parameters	Value
Q _i R _i P _i	diag(50,25,10) 10
E _i H _i	[-618 -757 171] diag(100,10,100,10) 200

Simulation results

In this section, the numerical simulations are designed and performed in the joint simulation platform of MATLAB/Simulink and TruckSim. The optimization problem in this paper is solved by the MATLAB function "fmincon." Note that there are many methods to reduce the computation time of optimization problem, such as particle swarm optimization,³⁸ alternating direction method of multipliers,³⁹ and etc. In the TruckSim, the truck type in the platoon is selected as "TS 2A-LCF Van Loaded."

A platoon is considered which consists of four trucks (i.e. one leading truck and three following trucks) with

(60)

the predecessor-leader communication topology. Note that the leading vehicle is a human-driven truck, that is, the leading truck can be guaranteed safe driving on both straight and curved roads. The trucks in the platoon have the same parameters, which are shown in Table 3. The prediction horizon is $R_H = 10$. The desired spacing is set to $d_0 = 16m$, and the penalty matrices are shown in Table 4.

Two simulation scenarios are established to validate the proposed integrated control scheme:

(1) Highway scenario: the allowed driving velocity range is between 17 and 24 m/s, the width of a single lane is 3.75 m, and the road curvature satisfies $|c_i| \le 0.0025$.

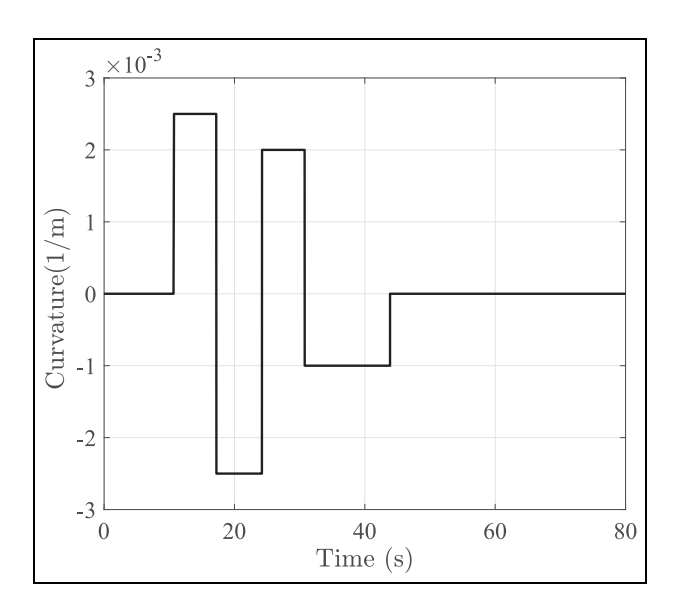


Figure 5. The road curvature for proposed controller of highway scenario.

(2) Medium and low velocity scenario: the allowed driving velocity range is between 10 and 17 m/s, the width of a single lane is 3.5 m, and the road curvature satisfies $|c_i| \le 0.01$.

In two scenarios, different road friction coefficients and road curvature are chosen to test the robustness of the proposed control scheme. In both longitudinal and lateral controller designs, constraints are selected as: $e_i^s \in [-2, 2], e_i^v \in [-2, 2], a_i \in [-2, 2], e_i^v(t) \in [-0.55, 0.55].$

Remark 2. In this paper, the control horizon and the prediction horizon are set to the same values. The prediction horizon (R_H) is usually determined by trial and error.⁴⁰

Highway scenario

The curvature of a road is shown in Figure 5 where the maximum road curvature is 0.0025. The initial velocity of the leading truck is $v_0^x = 25m/s$ and the desired velocity is given by

$$v_0^x = \begin{cases} 25 & m/s & t \le 10s \\ 20 - t & m/s & 10s < t \le 15s \\ 20 & m/s & 15s < t \le 50s \\ 20 + 0.7t & m/s & 50s < t \le 60s \\ 27 & m/s & 60s < t \end{cases}$$

and the initial velocity of the following trucks are $v_1^x = 26m/s$, $v_2^x = 24m/s$, and $v_3^x = 25m/s$. The initial velocity errors are $e_1^v = -1m/s$, $e_2^v = 1m/s$, and $e_3^v = 0m/s$. The initial longitudinal positions of trucks are $s_0 = 48m$, $s_1 = 32m$, $s_2 = 16m$, and $s_3 = 0m$, and the initial longitudinal position errors are $e_i^s = 0m$. The initial lateral position errors and heading errors of following trucks are $e_i^v = 0m$ and $e_i^\varphi = 0rad$. The road friction is set to 0.85.

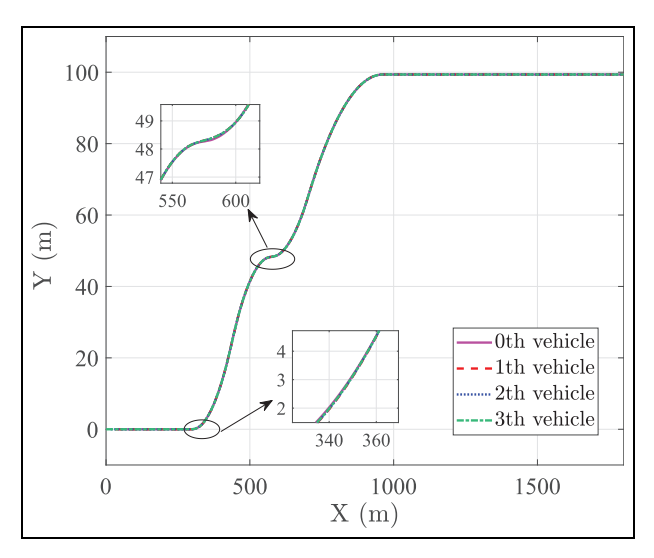


Figure 6. Trajectory of 4-vehicles platoon under highway scenario, the road adhesion coefficient is 0.85.

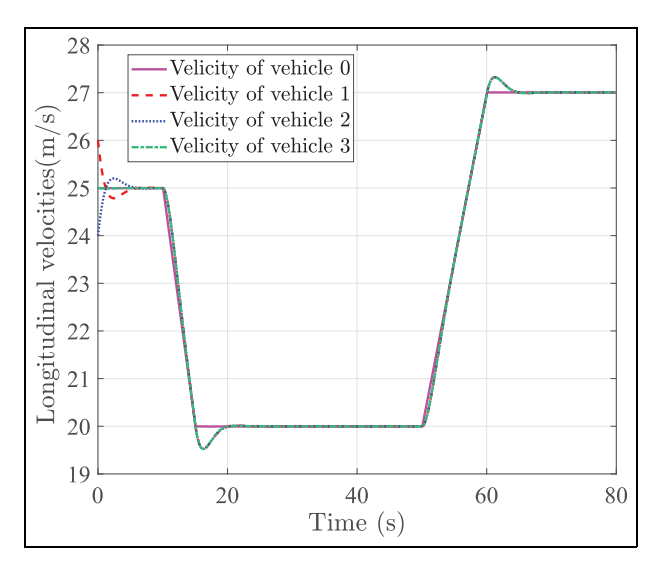


Figure 7. Longitudinal velocity of the trucks under the proposed longitudinal and lateral controller, the road adhesion coefficient is 0.85.

Simulation results using the presented integrated control framework are shown in Figures 6 to 12. The trajectory of all trucks is shown in Figure 6. It can be observed that all vehicles in the platoon converge to the reference path. Figures 7 and 8 show that the following trucks can quickly follow the velocity of the leading truck and the longitudinal position errors converge to zero, although there exists the initial state errors and the velocity of the leading truck changes during 5–10 s. With the fluctuation of velocity of the leading truck, the longitudinal velocity and longitudinal position error of each following truck also fluctuates, and the platoon achieves consensus in finite time. Furthermore, the longitudinal velocities and the longitudinal position errors are not obviously affected by the curvature. Figures 9 and 10 show that the lateral position errors

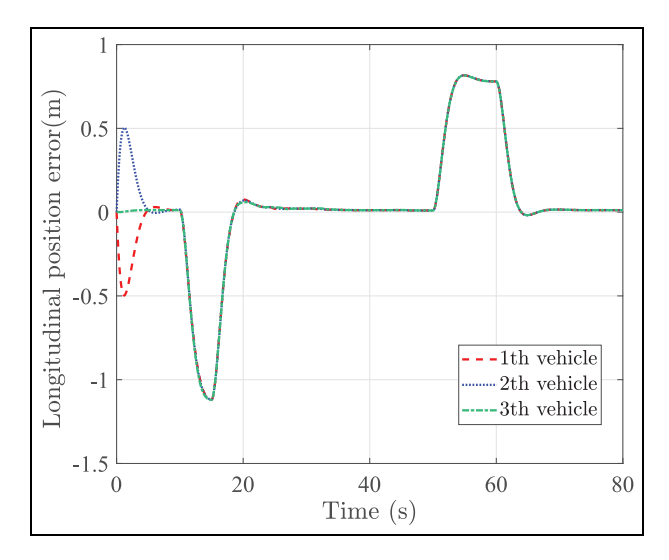


Figure 8. Longitudinal position error of following trucks under the proposed longitudinal and lateral controller, the road adhesion coefficient is 0.85.

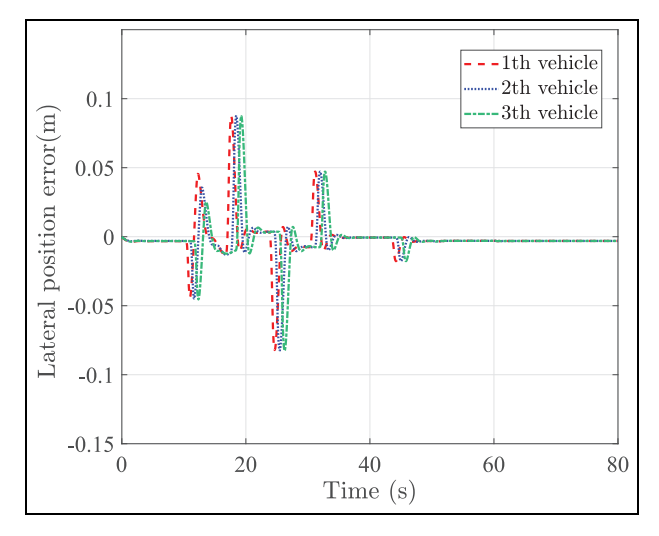
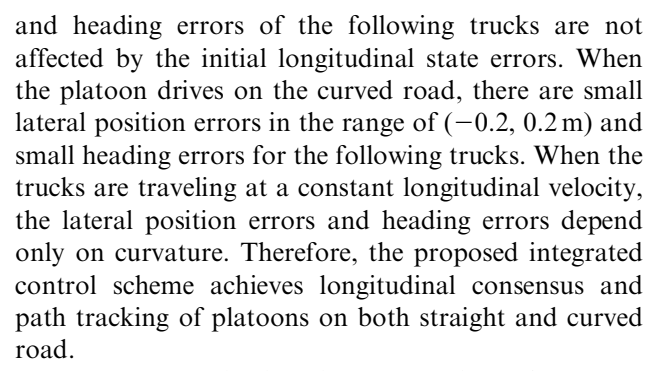


Figure 9. Lateral position error of following trucks under the proposed longitudinal and lateral controller, the road adhesion coefficient is 0.85.



In Figure 11, the first following vehicle decelerates and the second following vehicle accelerates at the initial moment due to the presence of the initial velocity error. The actual accelerations of the vehicles satisfy

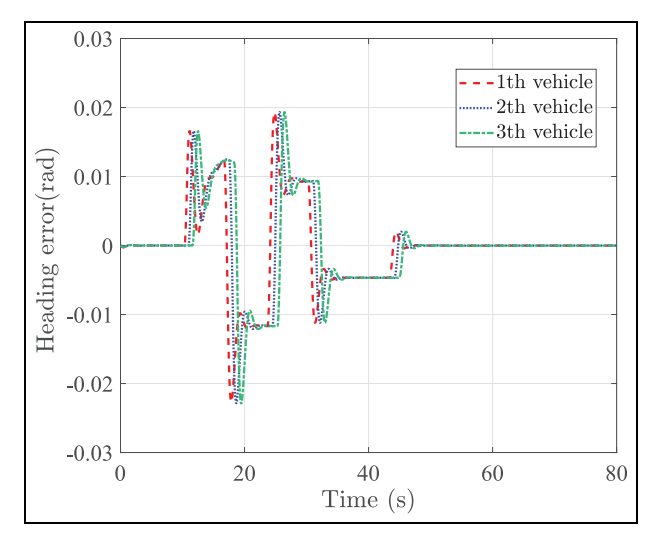


Figure 10. Heading error of following trucks under the proposed longitudinal and lateral controller, the road adhesion coefficient is 0.85.

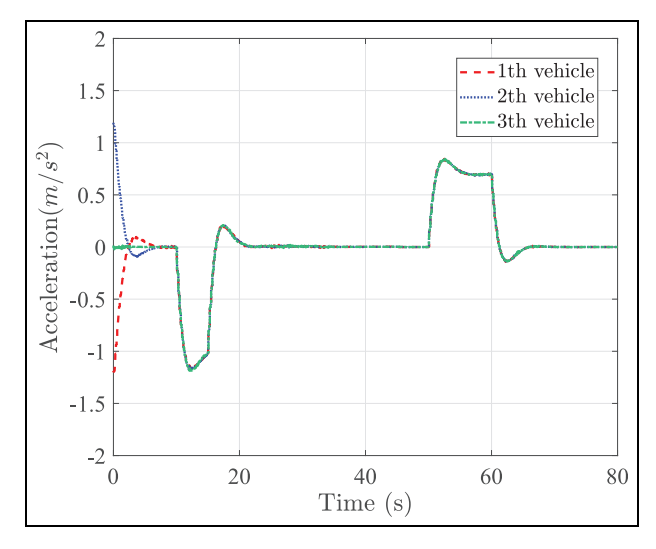


Figure 11. Acceleration under highway scenario, the road adhesion coefficient is 0.85.

the constraints. The front wheel angle of the vehicle is shown in Figure 12, which is in the range of $(-2^{\circ}, 2^{\circ})$.

Medium and low velocity scenario

An H_{∞} lateral controller is designed for comparison with the lateral controller proposed in this paper.⁴¹ The curvature of road is shown in Figure 13 where maximum road curvature is 0.01. The road friction is set to 0.35. The initial velocity of the leading truck is $v_0^x = 13m/s$ and the desired velocity is given by

$$v_0^x = \begin{cases} 17 & m/s & t \le 5s \\ 17 - t & m/s & 5s < t \le 7s \\ 15 & m/s & 7s < t \end{cases}$$

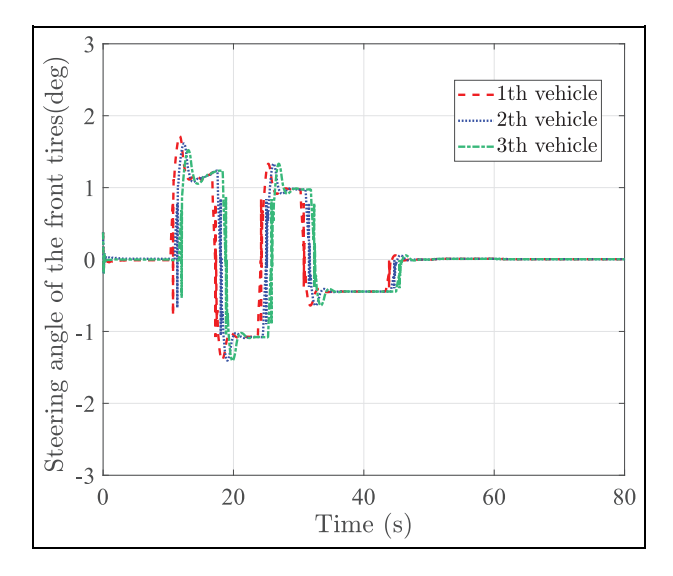


Figure 12. Steering angle of the front tires under highway scenario, the road adhesion coefficient is 0.85.

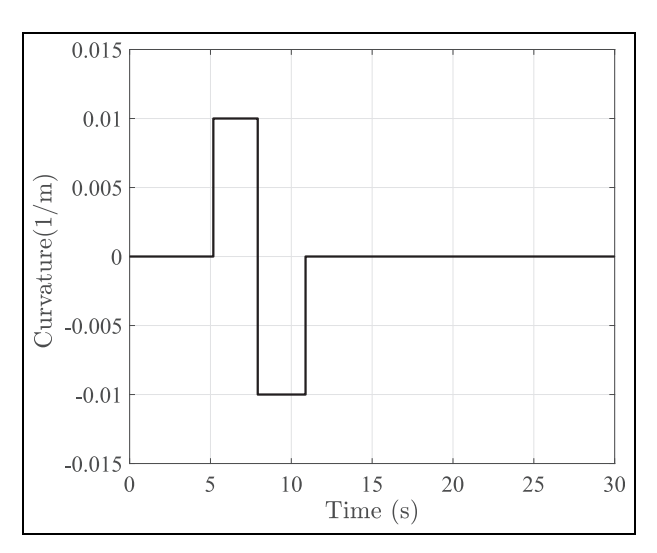


Figure 13. The road curvature of medium and low velocity scenario.

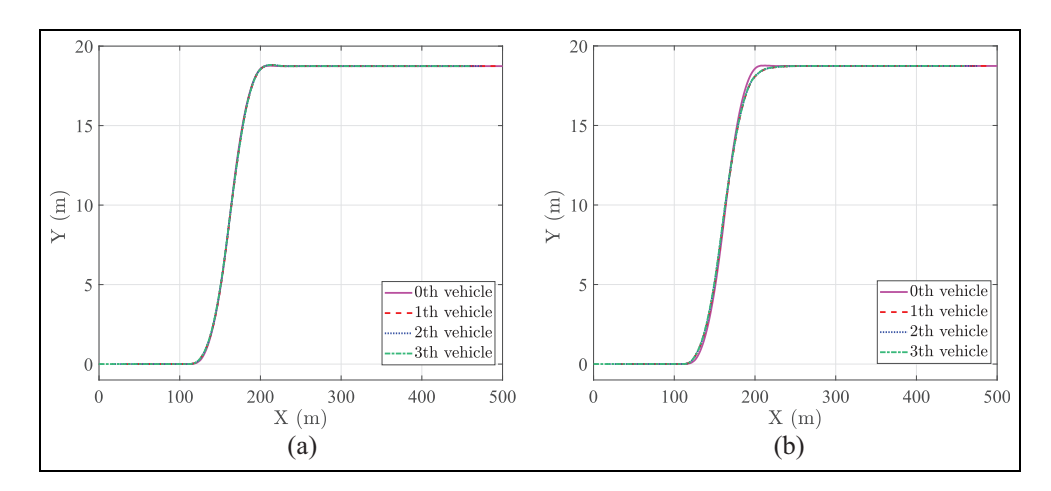


Figure 14. Trajectory of 4-vehicles platoon, the road adhesion coefficient is 0.35: (a) proposed lateral controller and (b) H_{∞} lateral controller.

the initial velocity of the truck i is $v_i^x = 17m/s$, i = 1, 2, 3. The initial velocity error of the truck i is $e_i^v = 0m/s$, i = 1, 2, 3. The initial longitudinal position of each truck in the platoon is $s_0 = 48m$, $s_1 = 32m$, $s_2 = 16m$, and $s_3 = 0m$, respectively. The initial longitudinal position error of the following truck i are $e_i^s = 0m$, i = 1, 2, 3. The initial lateral position error and the heading error of the following truck i are $e_i^v = 0m$ and $e_i^\phi = 0rad$, i = 1, 2, 3.

Simulation results using the presented integrated control framework are shown in Figures 14 to 20. The trajectory of all trucks is shown in Figure 14. Figures 15 and 16 show that, with the changes of the velocity of the leading truck, both the longitudinal velocity and the longitudinal position error of each following truck converge to the desired value under the proposed scheme. Figures 17 and 18 show the lateral position error and the heading error. The lateral position error under H_{∞} lateral controller indicates that the trucks exceed the

road boundary, which might collide with trucks in adjacent lanes and result in traffic accidents. However, under the proposed robust controller, the trucks drive within the road boundary.

Figure 19 shows that the acceleration of following trucks. At the time instants when the curvature of the road changes, there are significant fluctuations in Figure 19(b), because the lateral and longitudinal dynamics are coupled. The proposed lateral controller could reduce the effect on longitudinal acceleration and improve ride comfort.

Conclusions

This paper proposed an integrated longitudinal and lateral control framework for vehicle platoons with the predecessor-leader communicate topology. The coupled dynamics of vehicles was established where an error

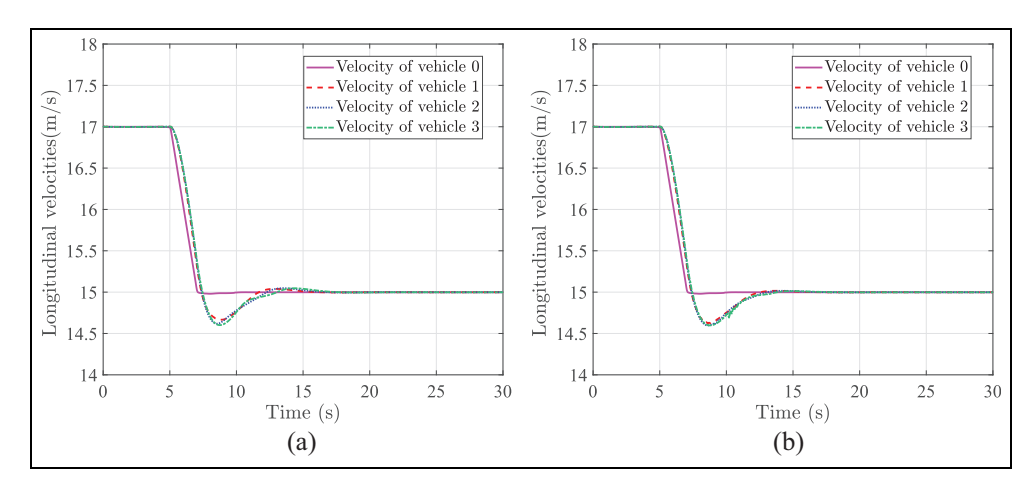


Figure 15. Longitudinal velocity of the trucks under medium and low velocity scenario, the road adhesion coefficient is 0.35: (a) proposed lateral controller and (b) H_{∞} lateral controller.

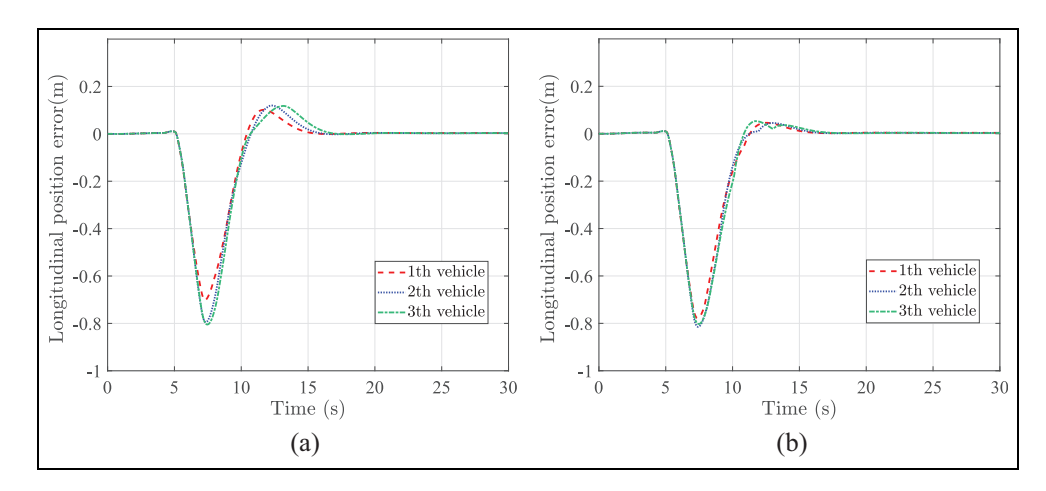


Figure 16. Longitudinal position error of following trucks under medium and low velocity scenario, the road adhesion coefficient is 0.35: (a) proposed lateral controller and (b) H_{∞} lateral controller.

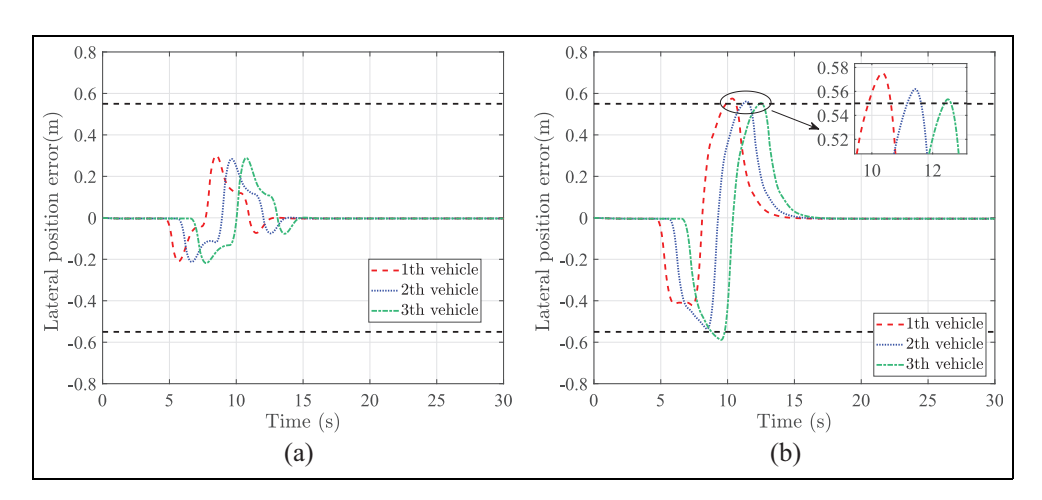


Figure 17. Lateral position error of following trucks under medium and low velocity scenario, the road adhesion coefficient is 0.35: (a) proposed lateral controller and (b) H_{∞} lateral controller.

model was established to describe the longitudinal deviations between the desired and actual value of the following vehicles, and the longitudinal velocity is treated as a varying parameter in the lateral dynamic model. Based on the error model, a DMPC algorithm with a terminal inequality constraint is proposed to

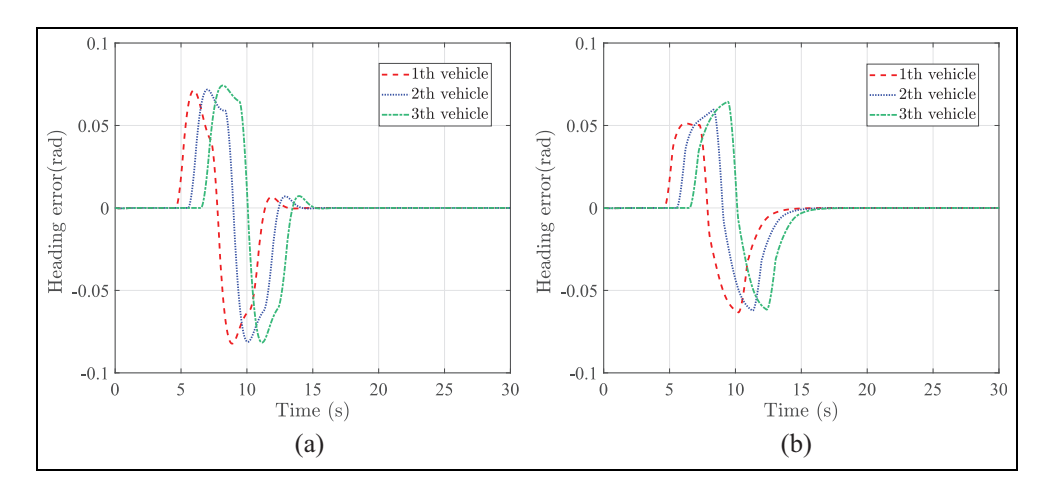


Figure 18. Heading error of following trucks under medium and low velocity scenario, the road adhesion coefficient is 0.35: (a) proposed lateral controller and (b) H_{∞} lateral controller.

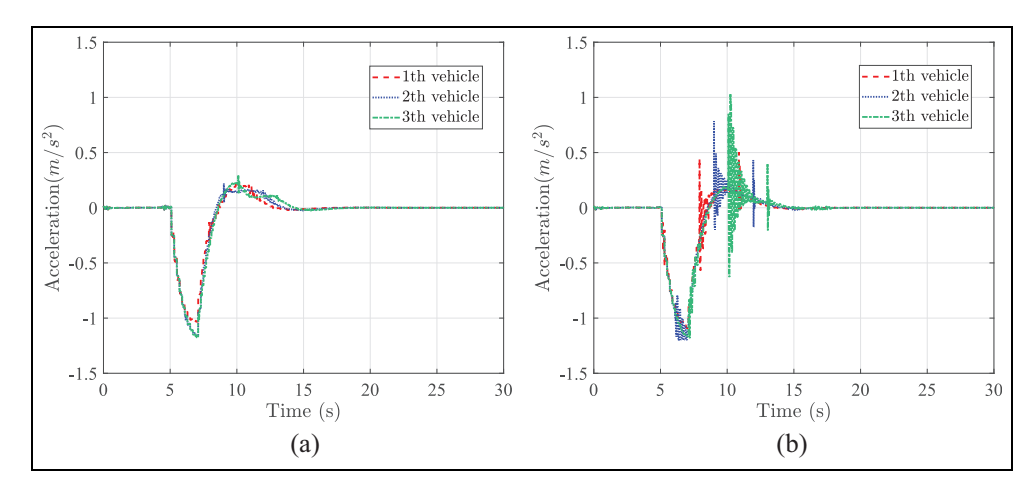


Figure 19. Acceleration of following trucks under medium and low velocity scenario, the road adhesion coefficient is 0.35: (a) proposed lateral controller and (b) H_{∞} lateral controller.

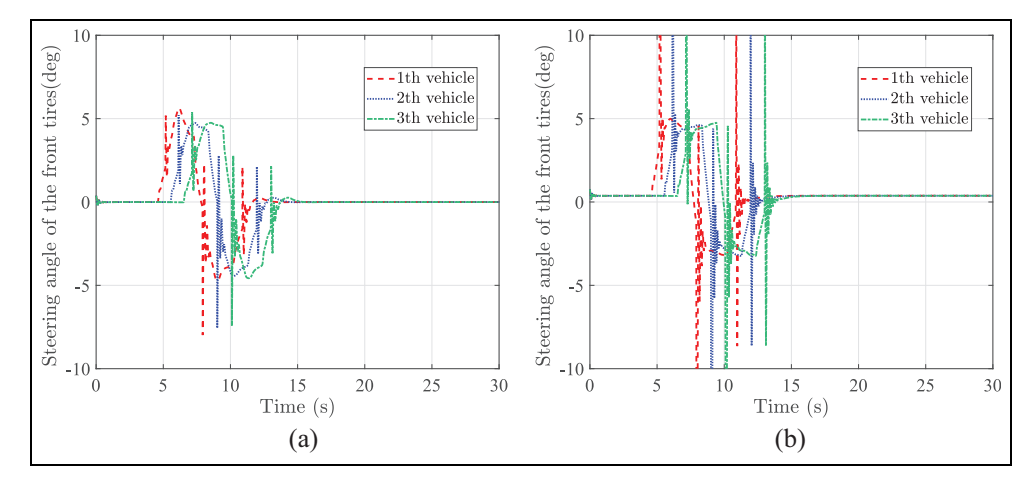


Figure 20. Steering angle of the front tires under medium and low velocity scenario, the road adhesion coefficient is 0.35: (a) proposed lateral controller and (b) H_{∞} lateral controller.

guarantee the longitudinal asymptotic consensus of vehicle platoons. Based on the lateral dynamics model,

a feedforward and robust feedback control strategy was adopted to ensure that vehicles in the platoon to

track the given path without offset. Simulation results in joint of MATLAB/Simulink and TruckSim verified the validity and robustness of the proposed framework. Future research will focus on the robust control of vehicle platoons to solve the problem about packet loss and communication delay.

Declaration of conflicting interests

The author(s) declared no potential conflicts of interest with respect to the research, authorship, and/or publication of this article.

Funding

The author(s) disclosed receipt of the following financial support for the research, authorship, and/or publication of this article: This work was supported by the National Natural Science Foundation of China (No.U1964202), the Science Foundation of Jilin Province (No.YDZJ202101ZYTS169), and the Foundation of Key Laboratory of Industrial Internet of Things and Networked Control (No.2019FF01).

ORCID iD

Shuyou Yu https://orcid.org/0000-0002-3258-6494

References

- 1. Li Y, Chen W, Peeta S, et al. Platoon control of connected multi-vehicle systems under V2X communications: design and experiments. *IEEE Trans Intell Transp Syst* 2020; 21(5): 1891–1902.
- 2. Qiang Z, Dai L, Chen B, et al. Distributed model predictive control for heterogeneous vehicle platoon with unknown input of leading vehicle. *Transp Res Part C Emerg Technol* 2023; 155: 104312.
- 3. Feng Y, Yu S, Chen H, et al. Distributed MPC of vehicle platoons with guaranteed consensus and string stability. *Sci Rep* 2023; 13(1): 10396.
- Zhang L, Hu M, Zhang H, et al. Channel-level event-triggered communication scheme for path tracking control of autonomous ground vehicles with distributed sensors. *IEEE Trans Veh Technol* 2023; 72(10): 12553–12566.
- Fiengo G, Lui DG, Petrillo A, et al. Distributed robust PID control for leader tracking in uncertain connected ground vehicles with V2V communication delay. *IEEE* ASME Trans Mechatron 2019; 24(3): 1153–1165.
- Luu DL, Lupu C and Alshareefi H. A comparative study of adaptive cruise control system based on different spacing strategies. J Control Eng Appl Inform 2022; 24(2): 3–12.
- Halder K, Gillam L, Dixit S, et al. Stability analysis with LMI based distributed H_∞ controller for vehicle platooning under random multiple packet drops. *IEEE Trans Intell Transp Syst* 2022; 23(12): 23517–23532.
- 8. Zhang CL and Guo G. Prescribed performance sliding mode control of vehicular platoons with input delays. *IEEE Trans Intell Transp Syst* 2024; 25(6): 11068–11076.

- 9. Yu S, Chen H, Feng Y, et al. Nash optimality based distributed model predictive control for vehicle platoon. *IFAC Pap OnLine* 2020; 53(2): 6610–6615.
- Negenborn R and Maestre J. Distributed model predictive control: an overview and roadmap of future research opportunities. *IEEE Control Syst Mag* 2014; 34(4): 87–97.
- 11. Mueller MA, Reble M and Allgoewer F. Cooperative control of dynamically decoupled systems via distributed model predictive control. *Int J Robust Nonlinear Control* 2012; 22(12): 1376–1397.
- 12. Giselsson P and Rantzer A. On feasibility, stability and performance in distributed model predictive control. *IEEE Trans Autom Control* 2014; 59(4): 1031–1036.
- Hu X, Xie L, Xie L, et al. Distributed model predictive control for vehicle platoon with mixed disturbances and model uncertainties. *IEEE Trans Intell Transp Syst* 2022; 23(10): 17354–17365.
- 14. Luu DL, Pham HT, Lupu C, et al. Research on cooperative adaptive cruise control system for autonomous vehicles based on distributed model predictive control. In: 2021 international conference on system science and engineering (ICSSE), Ho Chi Minh City, Vietnam, 26–28 August 2021, pp.13–18. New York: IEEE.
- Bai W, Xu B, Liu H, et al. Robust longitudinal distributed model predictive control of connected and automated vehicles with coupled safety constraints. *IEEE Trans Veh Technol* 2023; 72(3): 2960–2973.
- Zheng Y, Li SE, Li K, et al. Distributed model predictive control for heterogeneous vehicle platoons under unidirectional topologies. *IEEE Trans Control Syst Technol* 2017; 25(3): 899–910.
- 17. Li K, Bian Y, Li SE, et al. Distributed model predictive control of multi-vehicle systems with switching communication topologies. *Transp Res Part C Emerg Technol* 2020; 118: 102717.
- 18. Qiang Z, Dai L, Chen B, et al. Distributed model predictive control for heterogeneous vehicle platoon with intervehicular spacing constraints. *IEEE Trans Intell Transp Syst* 2023; 24(3): 3339–3351.
- 19. YanM, MaW, Zuo L, et al. Dual-mode control for platooning of connected vehicles with nonlinear dynamics. *Int J Control Autom Syst* 2019; 17(12): 3091–3101.
- Yang F, Wang H, Pi D, et al. Research on collaborative adaptive cruise control based on MPC and improved spacing policy. *Proc IMechE*, *Part D: J Automobile Engineering*. Epub ahead of print 6 April 2024. DOI: 10.1177/ 09544070241240166.
- Marino R, Scalzi S, Orlando G, et al. A nested PID steering control for lane keeping in vision based autonomous vehicles. In: 2009 American control conference, St. Louis, MO, USA, 10–12 June 2009, pp.2885–2890. New York: IEEE.
- Elbanhawi M, Simic M and Jazar R. Receding horizon lateral vehicle control for pure pursuit path tracking. J Vib Control 2018; 24(3): 619–642.
- Mata S, Zubizarreta A and Pinto C. Robust Tube-based model predictive control for lateral path tracking. *IEEE Trans Intell Veh* 2019; 4(4): 569–577.
- 24. Cao H, Song X, Zhao S, et al. An optimal model-based trajectory following architecture synthesising the lateral adaptive preview strategy and longitudinal velocity

- planning for highly automated vehicle. Veh Syst Dyn 2017; 55(8): 1143–1188.
- Sun H, Zhao H, Huang K, et al. A new approach for vehicle lateral velocity and yaw rate control with uncertainty. *Asian J Control* 2018; 20(1): 216–227.
- Kazemi A, Sharifi I and Talebi H. Longitudinal and lateral control of vehicle platoons using laguerre-based and robust MPC with merge and exit maneuvers. *Control Eng Pract* 2024; 142: 105737.
- Xu L, Zhuang W, Yin G, et al. Modeling and robust control of heterogeneous vehicle platoons on curved roads subject to disturbances and delays. *IEEE Trans Veh Technol* 2019; 68(12): 11551–11564.
- Kim J, Park JH and Jhang KY. Decoupled longitudinal and lateral vehicle control based autonomous lane change system adaptable to driving surroundings. *IEEE Access* 2021; 9: 4315–4334.
- dos Reis de Souza A, Efimov D and Rassi T. Robust output feedback MPC for LPV systems using interval observers. *IEEE Trans Autom Control* 2022; 67(6): 3188– 3195.
- 30. Atoui H, Sename O, Milans V, et al. LPV-based autonomous vehicle lateral controllers: a comparative analysis. *IEEE Trans Intell Transp Syst* 2022; 23(8): 13570–13581.
- 31. Wei S, Zou Y, Zhang X, et al. An integrated longitudinal and lateral vehicle following control system with radar and vehicle-to-vehicle communication. *IEEE Trans Veh Technol* 2019; 68(2): 1116–1127.
- Lan J, Zhao D and Tian D. Robust cooperative adaptive cruise control of vehicles on banked and curved roads with sensor bias. In: 2020 American control

- conference, Denver, CO, USA, 1–3 July 2020, pp.2276–2281. New York: IEEE.
- 33. Xiao L and Gao F. Practical string stability of platoon of adaptive cruise control vehicles. *IEEE Trans Intell Transp Syst* 2011; 12(4): 1184–1194.
- 34. Chen H and Allgwer F. A quasi-infinite horizon non-linear model predictive control scheme with guaranteed stability. *Automatica* 1998; 34(10): 1205–1217.
- Rajamani R. Vehicle dynamics and control. New York, NY: Springer-Verlag, 2011.
- Grimm G, Messina MJ, Tuna SE, et al. Examples when nonlinear model predictive control is nonrobust. *Automatica* 2004; 40(10): 1729–1738.
- Yu S, Reble M, Chen H, et al. Inherent robustness properties of quasi-infinite horizon nonlinear model predictive control. *Automatica* 2014; 50(9): 2269–2280.
- Zuo Z, Yang X, Li Z, et al. MPC-based cooperative control strategy of path planning and trajectory tracking for intelligent vehicles. *IEEE Trans Intell Veh* 2021; 6(3): 513–522.
- Krupa P, Jaouani R, Limon D, et al. A sparse ADMM-based solver for linear MPC subject to terminal quadratic constraint. *IEEE Trans Control Syst Technol*. Epub ahead of print 16 April 2024. DOI: 10.1109/TCST. 2024.3386062.
- 40. Rawlings J and Mayne D. *Model predictive control: the-ory and design*. Madison, WI: Nob-Hill, 2009.
- Boyd S, El Ghaoui L, Feron E, et al. *Linear matrix inequalities in system and control theory*. Philadelphia, PA: Society for Industrial and Applied Mathematics, 1994.